Time-Dependent Behavior of Cation Transport through Cellulose Acetate-Cationic Polyelectrolyte Membranes

Janina Hakanpää,[1] Kirsi Yliniemi,[1,*,z] Benjamin P. Wilson,[1,*] Matti Putkonen,[2] Sarah Höhn,[3] Eero Kontturi,[1] Sannakaisa Virtanen,[3,*] and Lasse Murtomäki[1]

[1]*Aalto University School of Chemical Engineering, FI-00076 Aalto, Finland*
[2]*VTT Technical Research Centre of Finland, 02044 VTT, Espoo, Finland*
[3]*Department of Materials Science and Engineering, Institute for Surface Science and Corrosion (LKO), Friedrich-Alexander-Universität Erlangen-Nürnberg, 91058 Erlangen, Germany*

Cation transport through a cellulose acetate-poly(N,N-dimethylaminoethyl methacrylate) membrane (CA:PDMAEMA) was studied with scanning electrochemical microscope (SECM) and the thickness increase of the membrane was monitored with ellipsometry. Upon addition of the polyelectrolyte PDMAEMA, the permeability of the probe cation (ferrocenium methanol, FcMeOH) was increased as much as 40-fold. Soaking membranes in an electrolyte solution doubled the permeability in plain CA membranes, whereas for PDMAEMA containing membranes the opposite was observed and the permeability was reduced by 20–40%. This time-dependent behavior is shown to be a result of the presence of PDMAEMA within the membrane matrix, thus providing an interesting platform for controllable membrane permeability.

 [DOI: 10.1149/2.1231802jes]

Manuscript submitted August 29, 2017; revised manuscript received December 13, 2017. Published February 2, 2018. This was Paper 929 presented at the New Orleans, Louisiana, Meeting of the Society, May 28–June 1, 2017.

In addition to the biological realm, membranes are used in numerous technical applications in everyday life: air filters, water purification, dialysis instrumentation, chemical synthesis etc. Moreover, the chemical composition of membranes can vary substantially, as shown by the existence of a wide range of different types of membranes such as polymer blends,[1] polymeric ion exchange,[2] electrospun fiber,[3] perovskite type ceramic[4] and liquid[5] membranes. Nevertheless, much of the research challenges in membrane technology are connected to the selective barrier properties of these materials, and in this communication, we study the permeability of cations through polymeric blend membranes.

The driving force of ionic transport is the gradient of the electrochemical potential[5] that can formally be divided into concentration (c_i) and Galvani potential (ϕ) contributions:

$$\vec{j}_i = -l_i \nabla \tilde{\mu}_i = -D_i \left(\nabla c_i + z_i f c_i \nabla \phi\right) \quad [1]$$

In the above equation, $\vec{j}_i$ is the flux density (mol cm^{-2} s^{-1}), D_i the diffusion coefficient and $\tilde{\mu}_i = \mu_i + z_i f \phi$ the electrochemical potential of an ion i; l_i is its ionic phenomenological coefficient, μ_i chemical potential and z_i charge number, and $f = F/RT$.

Equation 1 represents the Nernst-Planck approximation that is valid in moderately concentrated solutions (ionic strength < 1 M). Traditionally, transport through a membrane is considered to take place via the membrane pores. For porous membranes, in addition to the membrane thickness, pore size and pore density are the key factors that control the permeability. In contrast, for transport through nonporous (polymeric) membranes or membranes with a pore size $<$ 1 nm, a solution-diffusion mechanism is suggested.[3,6–8] In this model, solutes are first dissolved into the membrane matrix and then subsequently transferred through it. Partitioning of the solute between the solution and the membrane depends on properties, like their hydrophobicity, as well as the concentration (or pressure) of the solute. Transport through such membranes can also be enhanced by the carrier-facilitated mechanism[9] that commonly occurs in biological membranes where specific proteins can act as carriers.

Recently, we introduced a new membrane material made from a blend of cellulose acetate (CA) and poly(N,N-dimethylaminoethyl methacrylate) (PDMAEMA)[10,11] and this membrane proved to be particularly practical for the dissolution control of magnesium. The purpose of this paper is to study the behavior of the membrane in more detail; PDMAEMA is prone to water uptake and formation of hydrogels,[12–14] making it an interesting candidate as a membrane material, and thus, the possible applications of these membranes do not need to be limited only to the dissolution control of magnesium.

Cation transport was monitored with Scanning Electrochemical Microscopy (SECM), which enabled studies of membrane permeability. It is noteworthy that when using SECM, the effect of changes in thickness is removed from the permeability definition, thus revealing the inherent mobility ("diffusivity") of the material. The results show that addition of cationic polyelectrolyte PDMAEMA into the CA matrix enhances cation transport. Also, a time-dependent behavior - which has not been reported earlier for these membrane materials – was observed as the cation flow decreased as a function of time. Therefore, CA:PDMAEMA polymer blends are interesting materials for controlling cation flow, and this behavior can be attributed to the presence of PDMAEMA molecules.

Theory

The reaction kinetics at the SECM tip and substrate determines the shape of the approach curves. A kinetic barrier, such as a permeable membrane on a conductive substrate, deviates the tip current from that expected from an ideally conductive surface. In this paper, the model based on the works of Cornut and Lefrou[15–17] and Nogala et al.[18] have been utilized in the analysis of the approach curves. The equations presented by Nogala et al.[18] are used to fit the SECM data and the permeability is determined from the fitted data as previously shown by theoretical paper of Cornut and Lefrou;[15] thus, the following presentation of equations is based on these previous studies.[15–18]

The approach curves of the SECM tip toward the substrate are presented with normalized tip current vs. normalized distance, as outlined in Eqs. 2 and 3:

$$I_T = \frac{i_T}{i_{\text{bulk}}} \quad [2]$$

$$L = \frac{\min(z) - x + d_0}{r_T} \quad [3]$$

In Eqs. 2–3, i_T is the measured tip current and r_T tip radius; i_{bulk} is the tip current far from the substrate, z the distance between the

*Electrochemical Society Member.
zE-mail: kirsi.yliniemi@aalto.fi

tip and the substrate. Min (z) is the point where the tip contacts the substrate and d_0 the tilt of the tip (the definition of the tilt and Eq. 3 are described in more details by Nogala et al.[18]).

In addition to I_T and L, a parameter RG (i.e. ratio between the radius of the sealing glass capillary to the radius of Pt electrode) needs to be taken into account during the analysis.[15,18] The normalized tip currents for ideally insulating or conductive cases are given by Equations 4 and 5, respectively:[18]

$$I_T^{ins\ (L,\ RG)} = \frac{\frac{2.08}{RG^{0.358}}\left(L - \frac{0.145}{RG}\right) + 1.585}{\frac{2.08}{RG^{0.358}}\left(L + 0.0023RG\right) + 1.57 + \frac{\ln(RG)}{L} + \frac{2}{\pi RG}\ln\left(1 + \frac{\pi RG}{2L}\right)} \quad [4]$$

$$I_T^{cond}(L,\ \kappa,\ RG) = \alpha(RG) + \frac{1}{2\beta(RG)\xi(L,\ \kappa)} + \left[1 - \alpha(RG) - \frac{1}{2\beta(RG)}\right]\xi(L,\ \kappa) \quad [5]$$

where α and β are functions of RG as shown in the corresponding Equations 6 and 7, ξ is a function of κ and L as shown in Equation 8.[18]

$$\alpha(RG) = \ln(2)\left[1 - \frac{2}{\pi}\mathrm{acos}\left(\frac{1}{RG}\right) + \left(\frac{2}{\pi}\mathrm{acos}\left(\frac{1}{RG}\right)\right)^2\right] \quad [6]$$

$$\beta(RG) = 1 + 0.639\left[1 + \frac{2}{\pi}acos\left(\frac{1}{RG}\right)\right] - 0.186\left[1 - \left(\frac{2}{\pi}\mathrm{acos}\left(\frac{1}{RG}\right)\right)^2\right] \quad [7]$$

$$\xi(L,\kappa) = \frac{2}{\pi}\mathrm{atan}\left(L + \kappa^{-1}\right) \quad [8]$$

If the substrate is not fully insulating or conducting but the species formed on the tip is recovered on the substrate via an electrochemical reaction with the rate constant k, the tip current is governed by:[18]

$$I_T(L,\ \kappa,\ RG) = I_T^{cond}(L,\ \kappa,\ RG) + \frac{I_T^{ins}(L,\ RG) - 1}{\left(1 + 2.47RG^{0.31}L\kappa\right)\left(1 + L^{0.006RG+0.113}\kappa^{-0.236RG+0.91}\right)} \quad [9]$$

The dimensionless parameter κ is:

$$\kappa = \frac{kr_T}{D} \quad [10]$$

where D is the diffusion coefficient of the probe. The same formalism applies when an ideally conducting substrate is covered with a permeable film, see Supplementary Material. Assuming that the film is the only kinetic barrier, the permeability of the film can be related to the apparent rate constant ($k \rightarrow k_{app}$):[15]

$$k_{app} = \frac{P D_{film}}{\delta} = \kappa\frac{D}{r_T} \quad [11]$$

where P is the partition coefficient of the electroactive species between the film and the solution, D_{film} is the diffusion constant of the electroactive species in the film and δ is the thickness of the film. The product $PD_{film} = k_{app}\ \delta$ is called the permeability of the film,[15] although it has the dimension of a diffusion coefficient, i.e. it shows the effective diffusivity of ions through the membrane.

Experimental

Membranes were prepared on silicon wafers with poly(N,N-dimethylaminoethyl methacrylate) (PDMAEMA Polymer Source Inc, M_W 57700) and cellulose acetate (CA Sigma Aldrich, M_W 50000, DS 2.4155) blends in tetrahydrofuran (THF, Rathburn Chemicals Ltd, HPLC grade). 200 µl of the PDMAEMA:CA blend was pipetted on the silicon wafer and spin-coated at 1500 rpm for 90 s. The weight ratio of CA to PDMAEMA (CA:PDMAEMA) in the blend was either 1:0, 1:0.25 or 1:0.75. AFM images of the CA:PDMAEMA spin-coated silicon wafers in our previous studies[10] showed that addition of PDMAEMA smoothens the topographic featured of the surfaces.

Spin-coated wafers were immersed for approx. 5 min into ultrapure water after which the membranes were gently peeled off from wafer surface and used as a membrane. As the model system, we utilized a copper substrate covered with a CA:PDMAEMA membrane in an aqueous solution of ferrocene methanol (FcMeOH). Figure 1 shows the schematics of this model system, together with examples of tip response (i.e. feedback curves).

Transport of ions through the membranes was studied with SECM (CHI 900, USA). A platinum tip with diameter of 25 µm was sealed in a glass capillary ($RG \approx 6.5$, the ratio of the radii of the full tip including the glass sheath and the Pt electrode), the counter electrode was a Pt wire and a Ag/AgCl electrode acted as the reference. The Cu substrate was covered with a membrane and placed at the bottom of the cell. Tip current was recorded during the approach curves at regular intervals;

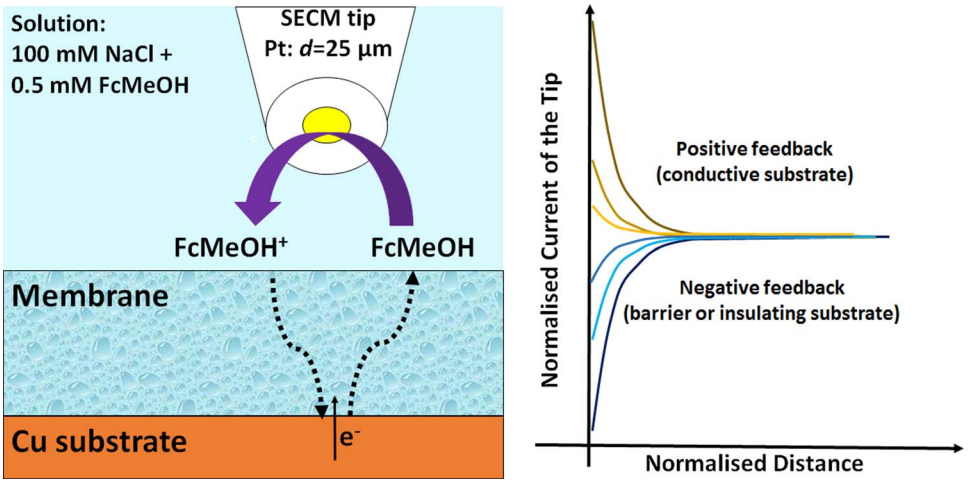

Figure 1. Left: schematics of the model system. Ferrocenemethanol (FcMeOH, a cation probe) was oxidized at the Pt electrode sealed in a glass capillary (SECM tip) and transported through the membrane; Right: The response of the tip (normalized current) can vary between ideally positive feedback and ideally negative feedback, depending on the barrier properties of the membrane placed on the top of the Cu substrate.

the tip potential was kept constant in the diffusion-controlled region of FcMeOH oxidation (0.4 V vs. Ag/AgCl).

The measurement solution was 0.5 mM FcMeOH (Aldrich) in 100 mM NaCl.

The results were fitted to Eq. 9 (Excel Solver) using a dimensionless rate constant κ, the tilt of the tip d_0 and the tip current far from the surface i_{bulk} as fitting parameters. As the fitting is very sensitive to the i_{bulk} changes, i_{bulk} was constrained to vary by a max. ± 1% from the measured value at the start of the fitted L range, while κ and d_0 were free fitting variables. Lowering further the error around i_{bulk} is not feasible as the detection limit of the equipment is at the pA level. The fitting range was from $L \approx 10$ until the point when the tip contacts the substrate surface (observed typically as a kink in the approach curve).

In order to calculate the permeability of membranes from SECM data, the thickness of the membranes was determined. The dry thickness of membranes spin-coated on silicon wafer was characterized with SEM (Hitachi TM-1000). Images of the cross-section were captured and the thickness was measured from 10 different spots; the average value was used for dry thickness.[11] The change in the thickness of spin-coated CA:PDMEAMA silicon wafers relative to their dry thickness was determined as a function of exposure time in a 100 mM NaCl solution at 20°C with single wavelength (632.8 nm) ellipsometry (SE400adv, Sentech Instruments GmbH). The measurements were performed at an angle of incidence of 70° and the data was fitted to the Cauchy model, using the dry-thickness value (from cross-section SEM) as a starting point and the refractive index n = 1.47.

FT-IR measurements (Thermo Scientific, Nicolet 6700 with an ATR-D cell: 32 scans between the 4000–650 cm^{-1}) were performed on membranes spin-coated on silicon wafer, before and after 24 h exposure to ultrapure water.

Results and Discussion

Figure 2 shows the approach curves measured after 30 mins and 3 h exposure to 0.5 mM FcMeOH + 100 mM NaCl solution. Solid lines represent the measurements with membranes (CA:PDMAEMA = 1:0, 1:0.25 or 1:0.75) and dotted lines are the fits of experimental data using Eq. 9.

As can be seen in Figs. 2a–2b, the experimental approach curves correlate very well with those from theory, indicating that the model chosen for the quantitative analyses is suitable for this system. All the approach curves show negative feedback, i.e. the membrane placed on the top of Cu substrate limits the transport of FcMeOH significantly. The pure copper surface displays almost ideally conductive behavior[19] and thus, the membrane shows itself as a kinetic barrier in the tip response. The k_{app} values calculated from the fits of the parameter κ to Eq. 10 are presented in Table I. Table I shows that k_{app} rises as the amount of PDMAEMA increases in the membrane. As can be observed, the k_{app} values of different membrane materials are distinctly different, in spite of any error that can contributed to i_{bulk}.

In order to study the actual permeability of the membrane, the thickness of the membrane was determined as a function of exposure time. Ellipsometer measurements (Figs. 3a and 3b) show that the thickness increase is clearly observable and the behavior of the distinct membrane materials show clear variations, both in terms of thickness

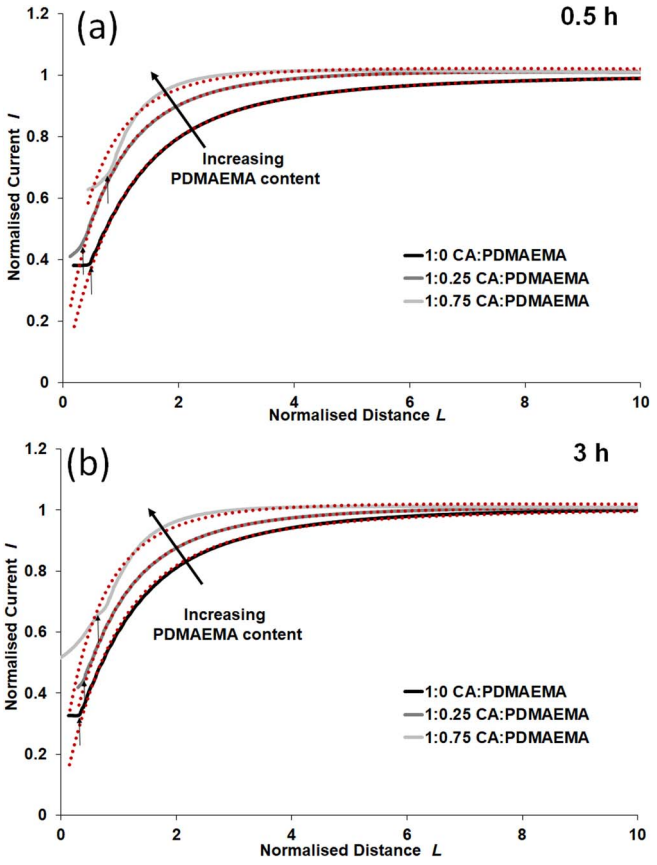

Figure 2. Approach curves on membrane covered Cu substrate in 0.5 mM FcMeOH + 100 mM NaCl. (a) Approach curves after 30 mins exposure to measurement solution and (b) after 3 h exposure to the measurement solution. Grey, solid lines are measurements and red dotted lines are fits to Eq. 9 and small arrows indicate the point-of-tip|surface contact.

and overall percentage increase. During the first 30 mins the thickness of the membranes display a similar increase, after which the membrane with the highest PDMAEMA content (1:0.75) experiences a further rapid and considerable change in thickness (in nm) while the 1:0 and 1:0.25 membranes follow a more similar trend. After 3 h exposure, the pure CA membrane had a thickness increase approx. 50 nm, the 1:0.25 membrane 60 nm, and the 1:0:75 membrane, 80 nm.

Using Equation 11, permeability ($PD_{film} = k_{app}\delta$) of the membranes can be determined from the k_{app} values (Table I) and thickness values determined from the ellipsometer data (Fig. 3a). Table II outlines the dry thickness of membranes, the thickness after exposure to 100 mM NaCl and the permeability of the membranes at two exposure times (after 0.5 h and 3 h exposure). As can be seen, the permeability of the membranes increases as much as 40-fold with an increasing amount of PDMAEMA, which is truly remarkable.

As the definition of permeability from SECM measurements ($PD_{film} = k_{app}\delta$) removes the effect of the thickness increase from the permeability value, the permeability presented here is a measure

Table I. The values of κ and k_{app} analyzed from approach curves in Fig. 2. The diffusion coefficient of FcMeOH in water is taken as 6.1 × 10^{-6} cm^2/s.[25]

	30 min exposure		3 h exposure	
CA:PDMAEMA	κ	k_{app} [cm/s]	κ	k_{app} [cm/s]
1:0	1.11×10^{-2} ($\pm 0.12 \times 10^{-2}$)	5.4×10^{-5} ($\pm 0.6 \times 10^{-5}$)	1.50×10^{-2} ($\pm 0.44 \times 10^{-2}$)	7.3×10^{-5} ($\pm 2.2 \times 10^{-5}$)
1:0.25	7.41×10^{-2} ($\pm 0.74 \times 10^{-2}$)	3.6×10^{-4} ($\pm 0.4 \times 10^{-4}$)	5.34×10^{-2} ($\pm 0.59 \times 10^{-2}$)	2.6×10^{-4} ($\pm 0.3 \times 10^{-4}$)
1:0.75	1.33×10^{-1} ($\pm 0.19 \times 10^{-1}$)	6.5×10^{-4} ($\pm 0.9 \times 10^{-4}$)	1.22×10^{-1} ($\pm 0.15 \times 10^{-1}$)	5.9×10^{-4} ($\pm 0.8 \times 10^{-4}$)

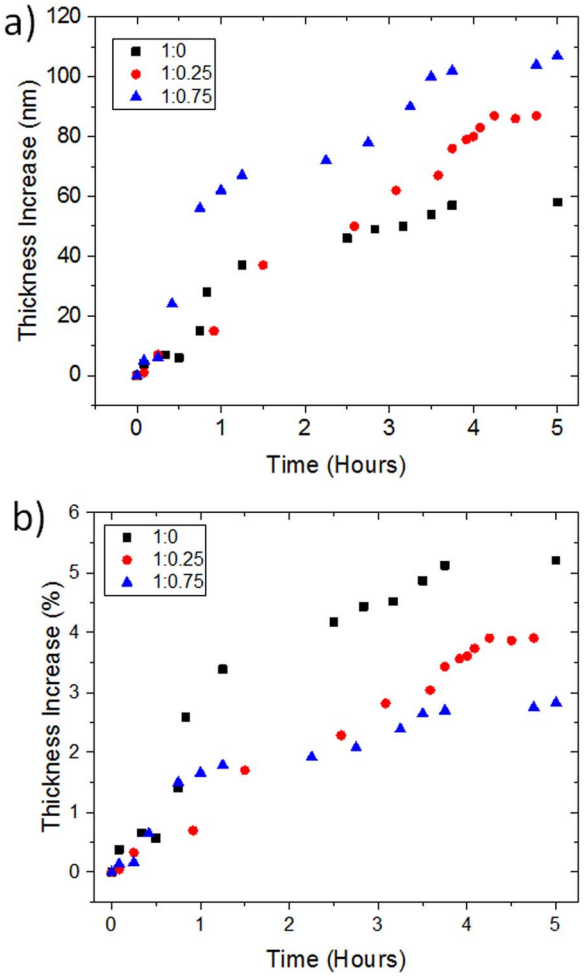

Figure 3. (a) Thickness increase (in mm) during the exposure to NaCl solution measured by ellipsometer, when the dry thickness was determined from the SEM image of the cross-section and (b) percentage change in thickness for the different film chemistries.

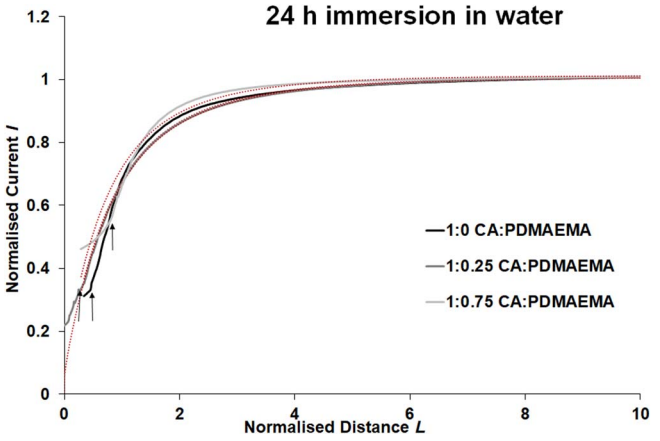

Figure 4. Approach curves on a membrane covered Cu substrate. Prior to measurements, the membrane was immersed in MQ water for 24 h after which the measurement was performed after 3 h exposure to measurement solution (0.5 mM FcMeOH + 100 mM NaCl). Grey, solid lines are measurements and red dotted lines are fits to Eq. 9 and small arrows indicate the point-of-tip|surface contact.

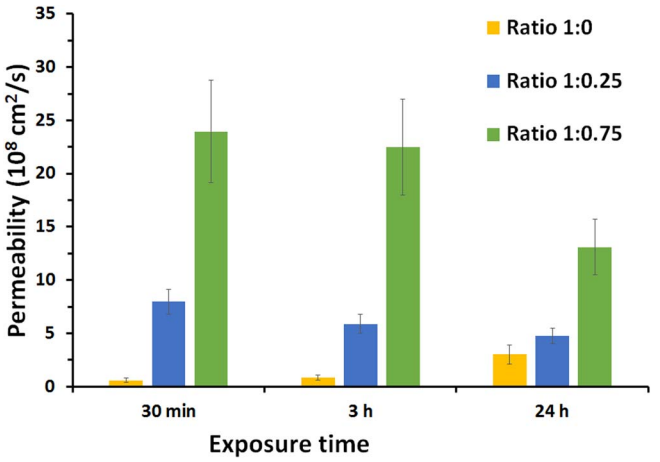

Figure 5. Permeabilities of different membranes at different exposure times, calculated by Eq. 11. The error bars are determined separately for each membrane type, using the error values obtained from i_{bulk} values in SECM data.

of the inherent mobility of a species ("diffusivity") within the membrane, primarily due to membrane characteristics like porosity, functional species etc. Therefore, the actual transport of cations through the CA:PDMAEMA can indeed be adjusted by PDMAEMA. The control of permeability of CA:PDMAEMA membranes is a very encouraging result if these polymer blend membranes are to be applied in the cation transport control.

Surprisingly, the membranes also show a time-dependent behavior of the permeability and this was studied also at longer exposure times, i.e. 24 h exposure. Figure 4 shows the SECM results (24 h in water + 3 h in 0.5 mM FcMeOH and 100 mM NaCl solution). As can be seen, the response of all the membranes looks very similar and all fitted k_{app} values vary between $2 \cdot 1^{-4} - 4 \cdot 1^{-4}$ cm/s (and the difference is less than the error due to $\pm$ 1% i_{bulk}). Nonetheless, one needs to take into account that the membranes have different thickness values and thus, permeability is determined from SECM and ellipsometer measurements in the same way as previously (thickness after 24 h exposure: 1:0 = 1.35 μm, 1:0.25 = 2.32 μm, 1:0.75 = 4.00 μm). Figure 5 displays the permeabilities of all the measurements together with error bars.

Figure 5 clearly demonstrates the time-dependent behavior of permeability and the difference between pure CA and PDMAEMA:CA membranes. At short exposure times the permeability of the 1:0.75 membrane is 40-fold higher than that determined for the pure CA membrane and even with longer exposure times it remains over 5 times greater. Moreover, the permeability trend is different for pure CA

Table II. Dry thickness of the films and the thickness and permeability of the films after exposure. Permeability of membranes calculated with Eq. 11: k_{app} values are from Table I and thickness values are determined from Fig. 2 at two exposure times.

	Dry thickness	Exposure time 30 min		Exposure time 3 h	
CA: PDMAEMA	δ [μm]	Δδ [nm]	Permeability [cm^2/s]	Δδ [nm]	Permeability [cm^2/s]
1:0	1.1	10	3.9×10^{-9}	50	8.4×10^{-9}
1:0.25	2.2	10	9.4×10^{-8}	60	5.9×10^{-8}
1:0.75	3.7	10	3.4×10^{-7}	80	2.7×10^{-7}

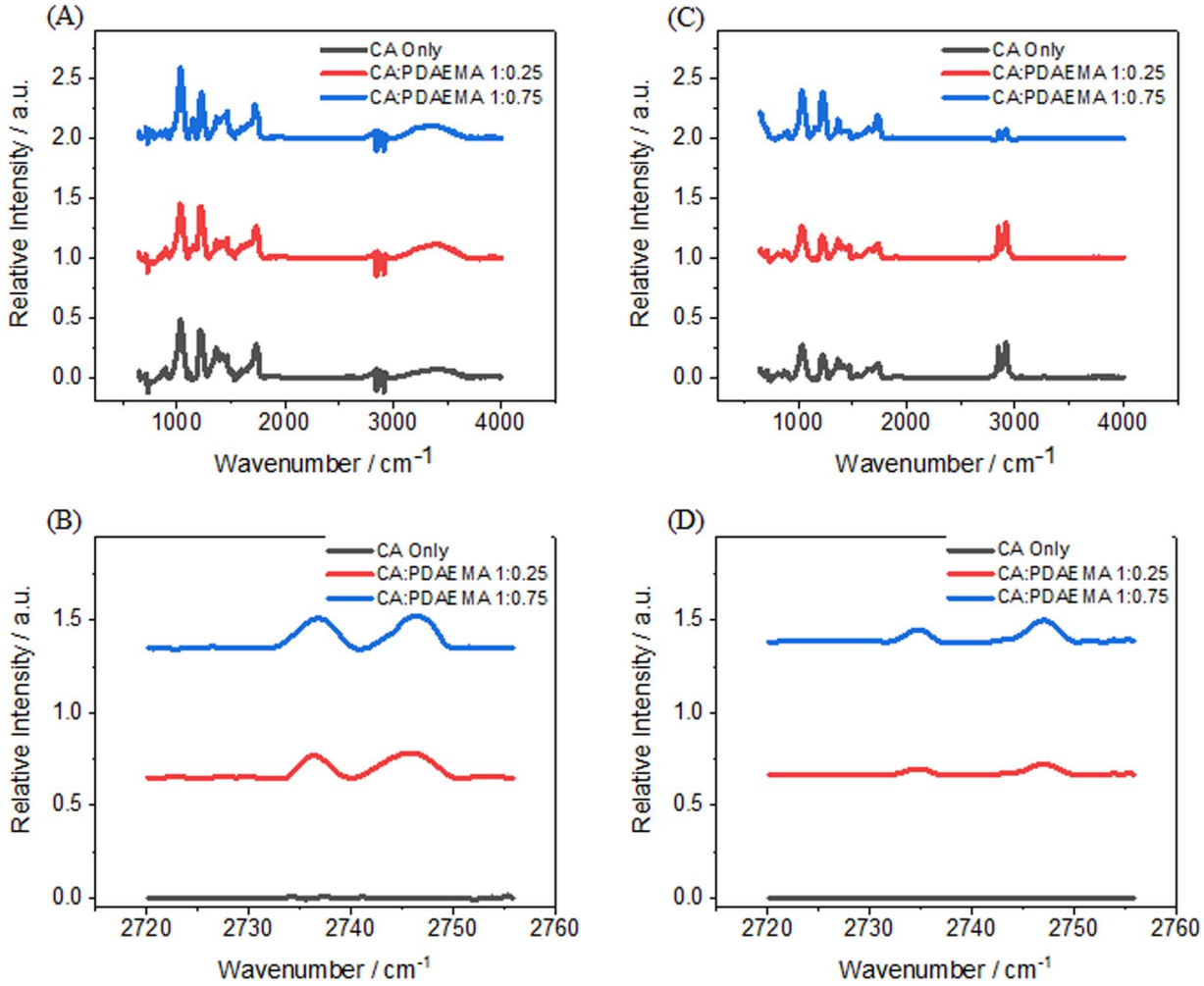

Figure 6. FT-IR measurements of CA:PDMAEMA membranes on silicon wafer before (A and B) and after (C and D) 24 exposure to water. Full spectra is shown in upper figures (A and C) while magnification at wavelength region characteristic for PDMAEMA is shown in lower figures (B and D).

membranes when compared to PDMAEMA membranes; in the case of pure CA membrane the permeability increases while for PDMAEMA containing membrane it decreases, and the decrease is as much as 20–40% during the first 3h. This trend remains true even when the largest error from the fitting of SECM data is used for each membrane types at all exposure times. It is noteworthy that such a time-dependent behavior has not been detected earlier for these CA:PDMAEMA membranes and actually, it could easily be overlooked without the capability of SECM and related theory developed by Cornut and Lefrou[15] which allows the removal of the thickness effect from the true "diffusivity" of the membranes.

Therefore, the observed time-dependent behavior is linked to the PDMAEMA molecules and is thus an effect of the membrane itself; the hindered diffusion or so called Renkin effect is known to result from a decrease in the pore diameter and/or increase in tortuosity of the membranes.[20] The reason for this hindered diffusion is the residual PDMAEMA left in the membrane, as FT-IR measurements (Fig. 6) show: the two peaks around 2700–2800 cm^{-1} are characteristic peaks of PDMEAMA, due to C-H stretching of $(CH_3)_2$-N.[21] Even if part of the PDMAEMA is dissolved from the membrane surface, clear peaks are still observed after 24 h exposure from PDMAEMA containing membranes, proving that there is still some PDMAEMA present in the membrane. Moreover, as the permeability trend is the opposite for pure CA membranes than for PDMAEMA containing membranes, it is evident that this effect is related to the behavior of PDMAEMA.

As mentioned earlier, PDMAEMA has a high ability to form hydrogels, which can swell as a response to different environmental triggers such as pH changes, redox potential changes, screening with low molecular salt, etc.[12–14] Therefore, it is highly probable that the remaining PDMAEMA molecules in the membrane (partly) block the diffusion pathways with a gel-like material when exposed to an aqueous environment, thus decreasing the permeability as a function of time.

The formation of hydrogel is more likely explanation than the electrostatic repulsion between the redox probe and PDMAEMA present in the membrane. The redox probe, FcMeOH, is oxidized to $FcMeOH^+$ at the SECM tip, after which it transfers across the membrane, which is slightly positively charged. Although this charge may impede or decelerate the rate of transfer, the overall effect of charges is assumed to be negligible as the ionic strength of the solution is 0.1 M, which makes the thickness of the electric double layer of the order of 1 nm only.[22] Therefore, the supposition of equal diffusion coefficients for the two ferrocene species should be reasonable.

This clearly PDMAEMA related behavior could be used in further membrane development. Previous studies have shown that using PDMAEMA based block-copolymers as additives in polyethersulfone polymer blend membranes provides an ability to change the permeability as a response to pH or ionic strength changes.[23,24] These earlier studies, however, have used water permeation tests for permeability determination, and thus any changes in thickness will also affect the result, while in contrast, the results presented here show that the nature of PDMAEMA molecules indeed causes the permeability change.

Overall, the results presented in this paper suggests that the presence of cationic polyelectrolyte (PDMAEMA) within these

membranes can function as a controlling but not an inhibiting factor for cation transfer; due to presence of PDMAEMA, these types of membranes could be used in future as potentially stimuli-responsive membrane materials. Moreover, these results demonstrate that utilising SECM in membrane studies is indeed a powerful tool as the effect of thickness increase can be separated from the permeability changes.

Conclusions

In this communication, the permeability of a probe cation in CA:PDMAEMA membranes was studied, in order to tune the capability of the membranes to control (but not fully inhibit) cation transport. An interesting time-dependent behavior was observed for the very first time for the CA:PDMAEMA membranes as the permeability decreased as a function of exposure time and it is believed to take place due to the presence of PDMAEMA in the membrane: the response of PDMAEMA to the aqueous solution decreases the pore diameter and/or increases tortuosity of the membranes. The use of SECM for permeability determination is critical in this case, as it separates the increased thickness from the actual transport of ions and thus, PDMAEMA molecules can be linked to this behavior. Therefore, the presence of PDMAEMA offers the possibility to develop stimuli-responsive membranes, which could use triggers such as pH and ionic strength in order to control the permeability of cations.

Notwithstanding, the permeability values measured for CA:PDMAEMA membranes were clearly higher than for membranes without PDMAEMA (i.e. pure CA membranes); with a 40-fold increase in permeability observed between pure CA and PDMAEMA containing membranes. Consequently, the results show that CA:PDMAEMA membrane is a promising material for applications where cation flow needs to be controlled.

Acknowledgments

Academy of Finland (JH, KY, BW, LM: Project No. 263 551, MP: Project No: 263 577, EK: Project No: 259 500) is acknowledged for the financial support of this work.

ORCID

Janina Hakanpää https://orcid.org/0000-0002-9269-4366
Kirsi Yliniemi https://orcid.org/0000-0003-2536-388X
Benjamin P. Wilson https://orcid.org/0000-0002-2874-6475
Matti Putkonen https://orcid.org/0000-0002-4166-2890
Sarah Höhn https://orcid.org/0000-0003-0071-9448
Eero Kontturi https://orcid.org/0000-0003-1690-5288
Sannakaisa Virtanen https://orcid.org/0000-0002-7179-7593
Lasse Murtomäki https://orcid.org/0000-0001-7667-4325

References

1. H. A. Mannan, H. Mukhtar, T. Murugesan, R. Nasir, D. F. Mohshim, and A. Mushtaq, "Recent Applications of Polymer Blends in Gas Separation Membranes," *Chem. Eng. Technol.*, **36**, 1838 (2013).
2. Y. S. Kim and K.-S. Lee, "Fuel Cell Membrane Characterizations," *Polymer Reviews*, **55**, 330 (2015).
3. F. E. Ahmed, B. S. Lalia, and R. Hashaikeh, "A review on electrospinning for membrane fabrication: Challenges and applications," *Desalination*, **356**, 15 (2015).
4. K. Zhang, J. Sunarso, Z. Shao, W. Zhou, C. Sun, S. Wanga, and S. Liu, "Research progress and materials selection guidelines on mixed conducting perovskite-type ceramic membranes for oxygen production," *RSC Adv.*, **1**, 1661 (2011).
5. K. Kontturi, L. Murtomäki, and J. A. Manzanares, *Ionic Transport Processes in Electrochemistry and Membrane Science*, Oxford University Press, (2008).
6. G. M. Geise, D. R. Paul, and B. D. Freeman, "Fundamental water and salt transport properties of polymeric materials," *Prog. Polym. Sci.*, **39**, 1 (2014).
7. J. S. Vrentas and C. M. Vrentas, "Transport in nonporous membranes," *Chemical Engineering Science*, **57**, 4199 (2002).
8. S. C. George and S. Thomas, "Transport Phenomena through Polymeric Systems," *Prog. Polym. Sci.*, **26**, 985 (2001).
9. Y. Li, S. Wang, G. He, H. Wu, F. Panab, and Z. Jiang, "Facilitated transport of small molecules and ions for energy-efficient membranes," *Chem. Soc. Rev.*, **44**, 103 (2015).
10. K. Yliniemi, B. P. Wilson, F. Singer, S. Höhn, E. Kontturi, and S. Virtanen, "Dissolution Control of Mg by Cellulose Acetate-Polyelectrolyte Membranes," *ACS App. Mater. Interfaces*, **6**, 22393 (2014).
11. J. Hakanpää, K Yliniemi, B. P. Wilson, M. Putkonen, E. Kontturi, S. Virtanen, and L. Murtomäki, *Study of Transport Properties of Polyelectrolyte-Cellulose Acetate Membranes*, *ECS Transactions*, **77**, 663 (2017).
12. J. Wei and L.-Y. Chu, Stimuli responsive cationic microgels and hydrogels based on poly(N,N-dimethylaminoethyl methacrylate): in book: Cationic Polymers in Regenerative Medicine, edited by S. Samal and P. Dubruel, *The Royal Society of Chemistry*, pp. 133–148 (2015).
13. A. Salama, M. El-Sakhawy, and S. Kamel, "Carboxymethyl cellulose based hybrid material for sustained release of protein drugs," *Int. J. Bio. Macromol.*, **93**, 1647 (2016).
14. Y. Cao, H. Liu, C. Fu, K. Li, L. Tao, L. Feng, and Y. Wei, "Thermo and pH Dual-Responsive Materials for Controllable Oil/Water Separation," *ACS Appl. Mater. Interfaces*, **6**, 2026 (2014).
15. R. Cornut and C. Lefrou, "Studying permeable films with scanning electrochemical microscopy (SECM): Quantitative determination of permeability parameter," *J. Electroanal. Chem.*, **623**, 197 (2008).
16. R. Cornut and C. Lefrou, "New analytical approximation of feedback approach curves with a microdisc SECM tip and irreversible kinetic reaction at the substrate," *J. Electroanal. Chem.*, **621**, 178 (2007).
17. R. Cornut and C. Lefrou, "New analytical approximations for negative feedback currents with a microdisk SECM tip," *J. Electroanal. Chem.*, **604**, 91 (2007).
18. W. Nogala, K. Szot, M. Burchardt, F. Roelfs, J. Rogalski, M. Opallo, and G. Wittstock,", *Analyst*, **135**, 2015 (2010).
19. K. Mansikkamäki, U. Haapanen, C. Johans, K. Kontturi, and M. Valden, "Adsorption of Benzotriazole on the Surface of Copper Alloys Studied by SECM and XPS," *J. Electrochem. Soc.*, **153**, B311 (2006).
20. K. A. Johnson, G. B. Westermann-Clark, and D. O. Shah, "Diffusion of charged micelles through charged microporous membranes," *Langmuir*, **5**, 932 (1989).
21. L. Jin, P. Liu, J. Hu, and C. Wang, "Synthesis of well-defined comb-like amphiphilic copolymers with protonizable units in the pendent chains: 2. Poly(2- (dimethylamino)ethyl methacrylate) grafted poly(methyl methacrylate-co-2-hydroxyethyl methacrylate) copolymers and their association behavior in aqueous solution," *Polymer International*, **53**, 142 (2004).
22. A. J. Bard and L. R. Faulkner, "*Electrochemical Methods: Fundamentals and Applications*, (2nd Ed.), John Wiley & Sons Inc, USA, 2001, pp 535.
23. Z. Yi, L.-P. Zhu, Y.-F. Zhao, Z.-B. Wang, B.-K. Zhu, and Y.-Y. Xu, "Effects of coagulant pH and ion strength on the dehydration and self-assembly of poly(N,N-dimethylamino-2-ethylmethacrylate) chains in the preparation of stimuli-responsive polyethersulfone blend membranes," *J. Membr. Sci.*, **463**, 49 (2014).
24. Z. Yi, L. P. Zhu, Y. Y. Xu, and X. L. Li, "F127-based multi-block-copolymer additives with poly(N,N-dimethylamino-2-ethylmethacrylate) end chains: the hydrophilicity and stimuli-responsive behavior investigation in polyethersulfone membranes modification," *J. Membr. Sci.*, **364**, 34 (2010).
25. P. Liljeroth, C. Johans, C. J. Slevin, B. M. Quinn, and K. Kontturi, "Micro ring-disk electrode probes for scanning electrochemical microscopy," *Electrochem. Commun.*, **4**, 67 (2002).